

## Supplementary Online Content

Bhattacharyya S, Wilson R, Appiah-Kusi E, et al. Effect of cannabidiol on medial temporal, midbrain, and striatal dysfunction in people at clinical high risk of psychosis: a randomized clinical trial. *JAMA Psychiatry*. Published online August 29, 2018. doi:10.1001/jamapsychiatry.2018.2309

### **eMethods.**

**eFigure 1.** CONSORT flow diagram

**eFigure 2.** Plot showing CBD plasma levels in placebo and CBD arms

**eFigure 3.** Acute effect of CBD on brain activation

### **eResults.**

**eTable 1.** Task-related activation during the encoding condition relative to baseline in healthy controls (n = 19)

**eTable 2.** Task-related activation during the recall condition relative to baseline in healthy controls (n = 19)

### **eDiscussion.**

### **eReferences.**

This supplementary material has been provided by the authors to give readers additional information about their work.

## **eMethods.**

The study protocol was approved by the National Research Ethics Service Committee London (Camberwell, St. Giles). All participants provided written informed consent. Recruitment started in July 2013 and was completed in October 2016. The study has been registered in the ISRCTN registry (ISRCTN46322781) and the protocol is available online (Supplementary Material 2- Protocol).

## **Subjects**

Thirty-three antipsychotic medication-naïve clinical high risk (CHR) participants were recruited from early intervention services for psychosis in South London<sup>13</sup>, Cambridge and West London (see Figure S1A for CONSORT diagram). CHR status was confirmed using the Comprehensive Assessment of At-Risk Mental States (CAARMS<sup>1</sup>) administered by an experienced research psychiatrist. Briefly, subjects met one or more of the personal assessment and crisis evaluation (PACE) criteria: (a) attenuated psychotic symptoms, (b) brief limited intermittent psychosis (BLIP, psychotic episode lasting <1 week that remits without treatment), or (c) recent functional decline and either schizotypal personality disorder or first-degree relative with psychosis. Nineteen age-matched ( $\pm$  3 years) healthy controls (HC) were recruited by local advertisement.

Individuals were excluded if there was a history of previous psychotic disorder or manic episode, neurological disorder or current DSM-IV diagnosis of substance dependence, IQ less than 70 and any contraindication to MRI or treatment with CBD. Psychopathology was measured using the CAARMS (positive and negative symptoms)<sup>1</sup> and state-trait anxiety inventory- state subscale (STAI-S)<sup>2</sup>, which was administered at baseline before drug administration. Finally, 2 CHR subjects were excluded, one from each of the CBD-treatment and placebo-treatment arms, after failing to correctly perform the imaging task, resulting in  $n=15$  participants in the CHR-CBD group and  $n=16$  in the CHR-PLB group.

## **Experimental procedure**

Using a parallel-group, double-blind, randomized and placebo-controlled design, CHR participants were randomized to either placebo (CHR-PLB) or CBD (CHR-CBD) treatment arms. Both CHR participants and researchers involved in data collection of CHR participants were blind to treatment allocation. A randomisation sequence was generated by STI pharmaceuticals across the two arms of the study using a blocking factor to ensure even distribution across the two arms. On recruitment of a study participant, an un-blinded clinical trial pharmacist, who was not involved with the rest of the study, allocated the participant to one of the two arms based on the randomisation list. On allocation, each participant became locked on to the specific treatment arm. Allocation information was kept concealed in the Maudsley hospital pharmacy.

Participants in the CHR-CBD arm received a single oral dose of 600mg of CBD, while those in the CHR-PLB arm were given a placebo capsule. The doses of antipsychotic medications that have previously been found to be effective in CHR patients (reviewed in<sup>3</sup>) have been comparable to their minimal effective dose in patients with established psychosis (reviewed in<sup>4</sup>). Therefore, we opted for the 600 mg/day dose of CBD for the present study based on previous evidence that CBD doses of 600-800 mg/day were as effective at reducing symptoms as antipsychotic medication (amisulpiride)<sup>5</sup> in patients with first-episode psychosis. Subjects then underwent functional magnetic resonance imaging (fMRI) whilst performing a verbal paired associate learning task lasting approximately 12 minutes. MRI scanning started 3 hours after the taking the study drug (CBD or placebo), as previous research has shown that CBD levels reached its peak around 3 hours following oral administration<sup>6</sup>. HC participants were investigated under identical conditions, except that they did not receive any study drug.

On the study day, all participants consumed a light standardised breakfast in front of the researchers, and were asked to have refrained from cannabis for 96 hours, alcohol for a

minimum of 24 and nicotine for 6 hours before scanning. Furthermore, they are asked not to have used any other recreational drugs for two weeks before the study day. A urine sample prior to scanning was used to screen for use of illicit drugs. Three hours prior to scanning, subjects in the CBD-CBD group received one cannabidiol capsule (600mg, approx. 99.9% pure, THC-Pharm, Frankfurt, Germany), whilst those in the CHR-PLB group received a visually identical flour (placebo) capsule.

### **Verbal paired associate learning task**

Inside the MRI scanner, subjects performed a verbal paired associate (VPA) learning task that we have previously used in conjunction with fMRI and pharmacological challenge<sup>7,8</sup>, including CBD administration<sup>9</sup>. It comprised 3 conditions (encoding, recall, and baseline), with stimuli presented visually in blocks. The accuracy of responses during each condition was recorded online. During the encoding condition, subjects were shown pairs of words printed on a pair of blue rectangles and were required to decide whether they went well together (to promote encoding), saying ‘yes’ or ‘no’ aloud after each pair. The same word pairs were presented in the encoding condition 4 times, so that the associations could be learned over repeated blocks. During the recall condition, one of the words from previously presented pairs was shown (printed similarly on a pair of blue rectangles of identical dimensions as in the encoding condition) and participants were asked to say the word that it had previously been associated with. Subjects said “pass” if they could not recall the missing word. During a baseline condition, participants viewed a pair of blank blue rectangles of identical dimensions as in the encoding/ recall condition.

Stimuli were presented in 40-second blocks of 8 stimulus pairs, with the 3 conditions presented in the same order (encoding, recall, and baseline) on 4 occasions. Within each encoding block, the order of the word pairs was randomized. A visual prompt preceded each encoding (“Do these words go well together?”) and recall block (“Which word was associated with this?”). Presenting the same encoding stimulus pairs 4 times across repeated blocks

permitted assessment of the effect of learning on activation and recall accuracy. The words presented were taken from the MRC (Medical Research Council) Psycholinguistic Database<sup>10</sup> and were similar in terms of number of letters, familiarity, written frequency, concreteness, imageability, and meaningfulness<sup>11</sup>. Participants were familiarized with the task during a training session with a set number of trials outside of the scanner using different words from those presented during imaging.

For each participant, the blood oxygen level–dependent haemodynamic (BOLD) response of the brain during each encoding and recall block, measured using a 3T MRI scanner, was contrasted with that during the baseline condition.

### **Image Acquisition**

Images were acquired using a 3T MRI scanner (GE Medical Systems, Milwaukee, Wisconsin). One hundred and forty seven T2\*-weighted volumes were acquired using a gradient echo sequence axially in 39 x 3mm slices with a 3.3mm slice gap running parallel to the intercommissural (AC–PC) plane (FOV 24×24 cm and matrix 64×64). A 30ms echo time, 90° flip angle, and compressed acquisition with a 2s repetition time and 3s silence was also used. A high-resolution inversion recovery image data set was acquired to facilitate anatomic localization of activation.

### **Data Analysis**

**Image analysis:** The fMRI data were analyzed with software developed at the Institute of Psychiatry, Psychology and Neuroscience (XBAM, version 4.1), using a nonparametric approach to minimize assumptions

(<https://www.kcl.ac.uk/ioppn/depts/neuroimaging/research/imaginganalysis/Software/XBAM.aspx>)<sup>12,13</sup> about the distribution of the data. In contrast to other commonly employed image analysis approaches, XBAM, in particular, does not assume a Gaussian population distribution of fMRI signals in the brain. This is an assumption that is very difficult to test in

small groups with neuroimaging data and when tested, is found to be violated<sup>12,13</sup>. Instead, XBAM employs median statistics and permutation-based rather than normal theory-based approaches for statistical inference. Therefore it is less sensitive to the effects of outlier values that may bias the distribution of the data<sup>14</sup>. In this method, the test statistic is computed by standardizing for individual differences in residual noise before embarking on a second-level, multi-subject testing, using robust permutation-based methods, employing a mixed-effects approach.

Images were corrected for subject motion<sup>15</sup> and spatially smoothed using a 7.2 mm full-width-at-half-maximum Gaussian filter to average the relative intensities of neighbouring voxels. Responses to the experimental paradigm were detected by convolving each component of the design with two gamma-variate functions (peaks at 4 and 8s) to model the blood oxygen level-dependent (BOLD) response. Then, using the constrained BOLD effects model, a best fit between the weighted sum of these convolutions and the change over time at each voxel was computed<sup>16</sup>. Following least-squares fitting of this model, a sum of squares (SSQ) ratio statistic was estimated at each voxel. This consisted of the ratio of the SSQ of deviations from the mean image intensity due to the model (over the whole time series), to the SSQ of deviations due to the residuals. These data were then permuted using a wavelet-based method described and characterized previously<sup>17</sup>, to determine significantly activated voxels specific to each condition. Activated voxels were then grouped into clusters using a method described before<sup>18</sup>, which has been shown to give excellent cluster-wise type 1 error control. SSQ ratio maps for each individual were transformed into standard stereotactic space<sup>19</sup> using a two-stage warping procedure<sup>12</sup> for the purpose of localization of activations. As a first step, an average image intensity map for each individual over the course of the experiment was computed. We then computed the transformations required to map this image to the structural scan for each individual and then from 'structural space' to the Talairach template by maximizing the correlation between the images at each stage. The SSQ ratio and BOLD effect size maps were then transformed into Talairach space using these transformations.

Group activation maps were computed for each group in each drug condition by determining the median SSQ ratio at each voxel (over all individuals) in the observed and permuted data maps. Medians were used to minimize outlier effects. The distribution of median SSQ ratios over all intracerebral voxels from the permuted data was then used to derive the null distribution of SSQ ratios, which allows group activation maps to be thresholded at the desired voxel or cluster-level type 1 error rate. This gave group activation maps for each condition that could be compared against each other using non-parametric repeated-measure analysis of variance (ANOVA)<sup>12</sup>. The voxel-wise statistical threshold was set at  $p=0.05$  and the cluster-wise thresholds were adjusted to ensure that the number of false positive clusters per brain would be  $<1$  (regions that survive this critical statistical threshold and the corresponding  $p$  values are reported). This excluded any areas of activation, which did not meet this threshold of significance. By conducting analyses at a cluster-level, data from more than one voxel is integrated into the test statistic giving greater sensitivity and it also allows for a reduction in the search volume or overall number of required tests for whole brain analysis. In comparison to analysis at the voxel level, cluster level analyses with a non-parametric approach thereby helps mitigate the multiple comparisons problem<sup>20</sup>.

The BOLD response in each subject was modelled using only trials associated with correct responses in the recall condition, and responses confirming attention to the task during encoding. To investigate the differences in brain activation between the CHR-PLB and HC subjects the respective group activation maps were contrasted using a between-group, non-parametric analysis of variance. Group activation maps for the CHR-CBD and CHR-PLB subjects were similarly contrasted using a between-group, non-parametric analysis of variance to investigate the effect of single dose of CBD on brain activation in CHR patients relative to placebo treatment. To test the hypothesis that activation in the CHR-CBD group would be intermediate between that of HC and CHR-PLB subjects, a non-parametric analysis of variance was performed to examine whether a linear relationship in brain activation (CHR-PLB  $>$  CHR-CBD  $>$  HC or CHR-PLB  $<$  CHR-CBD  $<$  HC) existed within the whole brain.

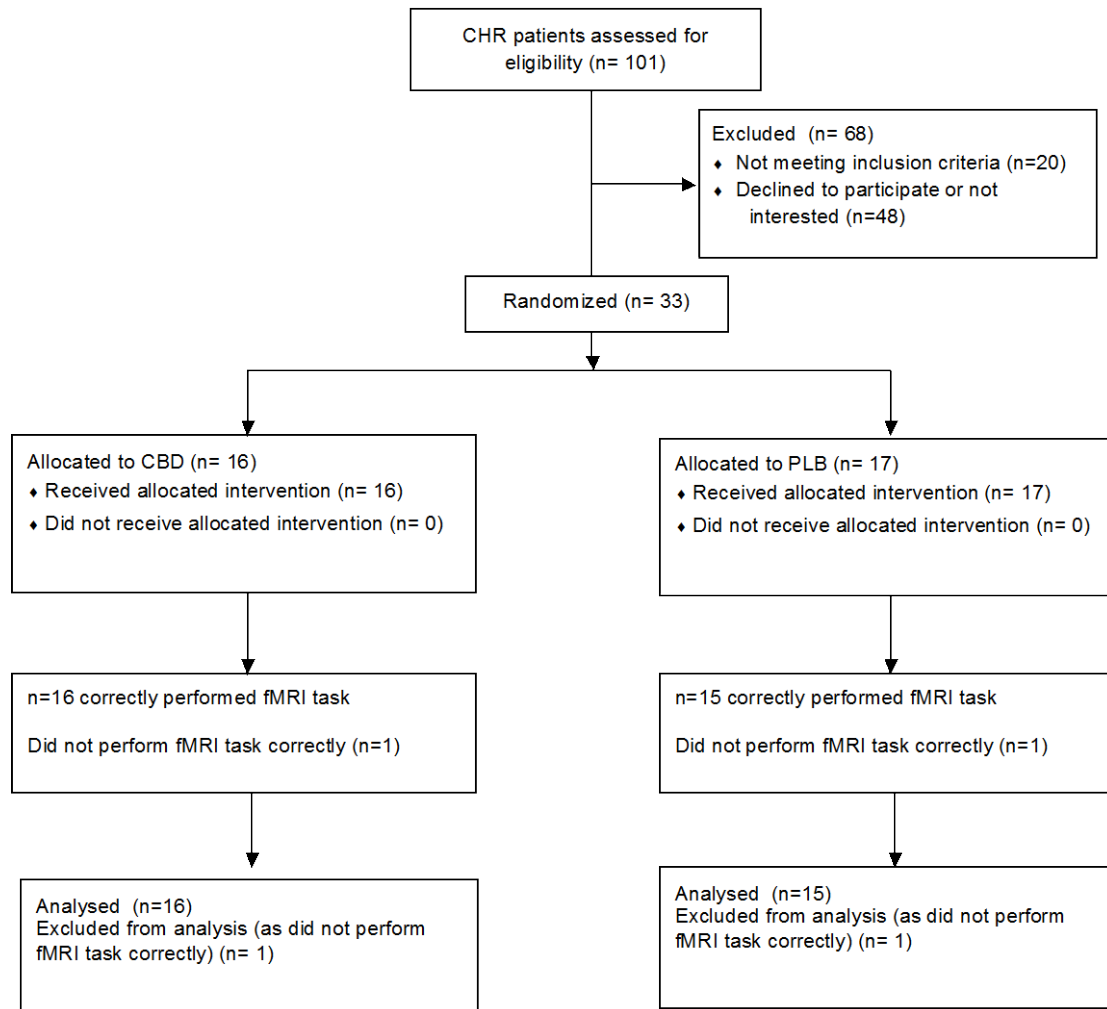
The statistical analyses used type I error control to obtain less than 1 false-positive cluster within the whole map.

**Task performance and symptom data analysis:** Recall performance was analysed using repeated-measures analysis of variance (SPSS version 22; SPSS Inc, Chicago, Illinois). Greenhouse-Geisser adjustment was applied where the assumption of sphericity was violated. Correlational analysis between recall performance and psychopathology (CAARMS positive symptom scores) and between psychopathology (CAARMS positive and negative symptom scores and STAI-S) and functional brain activation (midbrain and striatum) was conducted using Pearson's test (two-tailed unless otherwise specified). Categorical variables were compared with chi-square or fisher's exact test as appropriate. Continuous variables were compared with independent t tests.

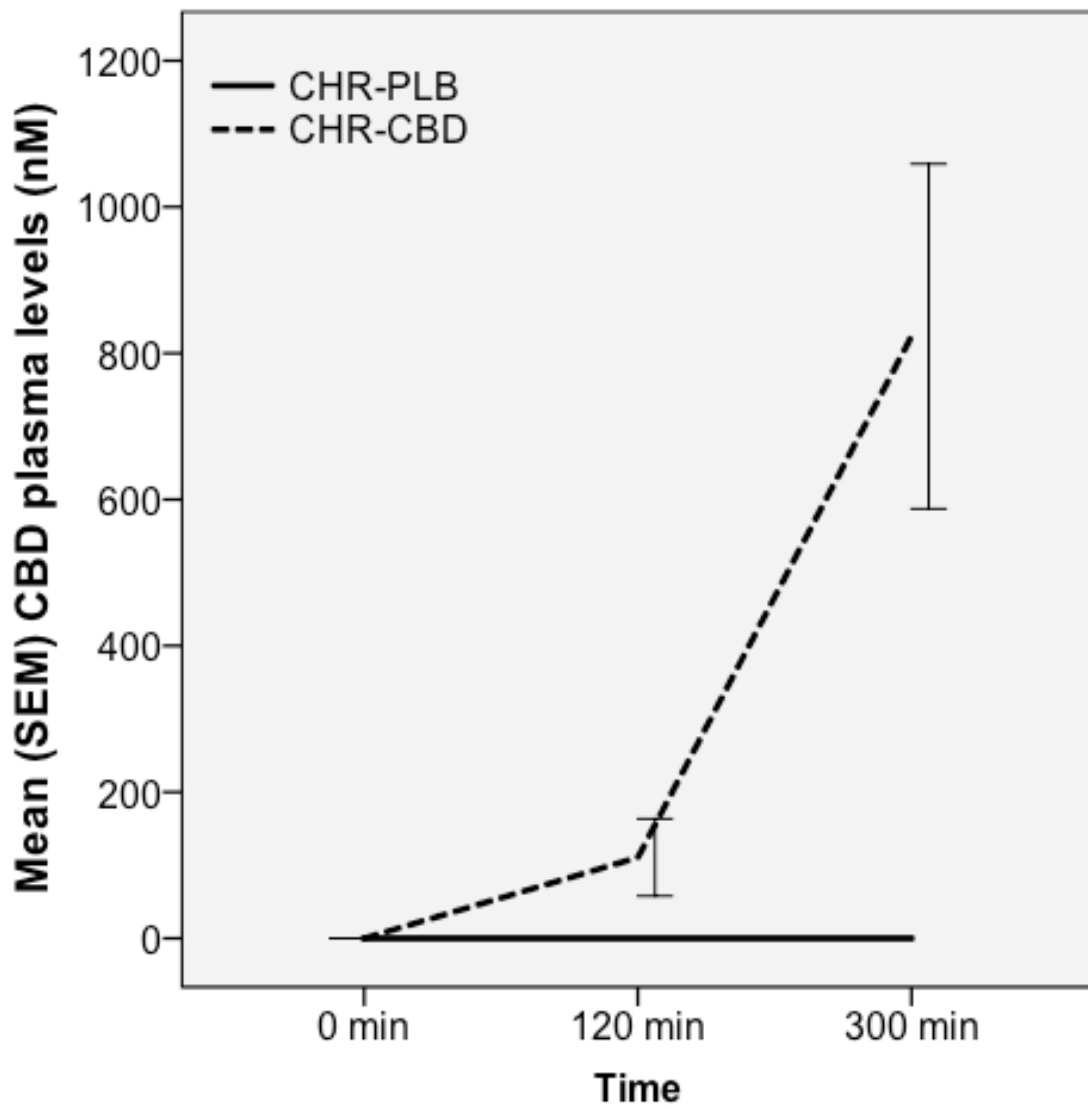
**Sample Size:** Based on our previous study in healthy volunteers using a repeated-measures, within-subject design, we estimated that a sample size of  $n=15$  would be required to detect differences between the placebo and CBD condition on neural activation with an alpha ( $\alpha$ ) of 0.05 at 90% power and an SD of 0.04 and anticipated minimal difference in means as 0.036<sup>9</sup>.



**eFigure 1.** CONSORT flow diagram



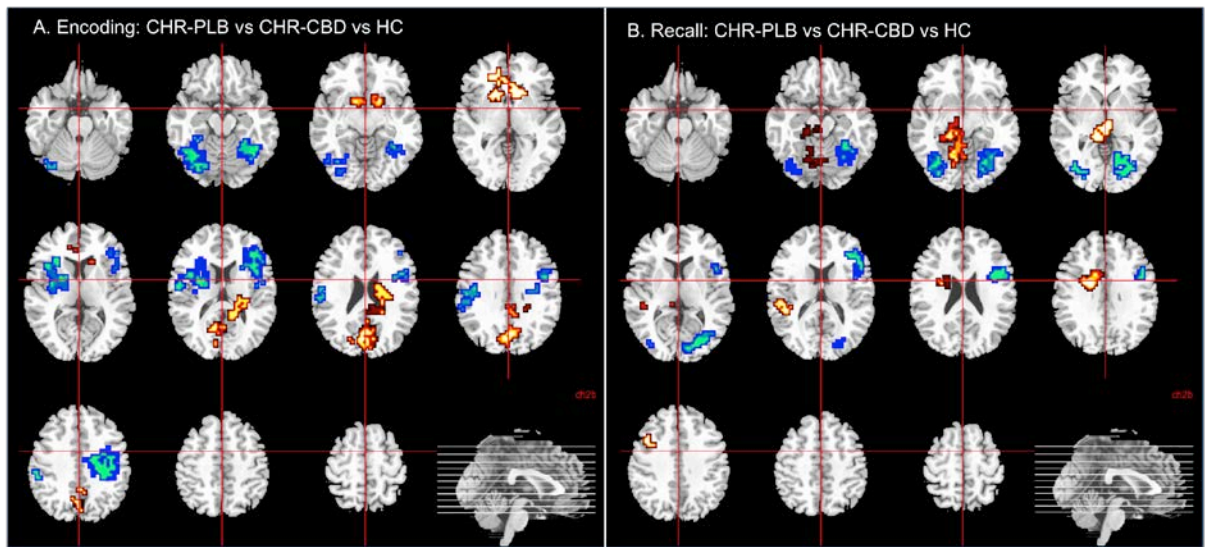
**eFigure 2.** Plot showing CBD plasma levels in placebo and CBD arms



**eFigure 3. Acute effect of CBD on brain activation**

Acute effect of CBD on brain activation relation to placebo treatment in CHR participants and healthy controls (CHR-PLB vs CHR-CBD vs HC; right side of the brain is shown in the right of the brain sections in all of the images; (CHR-PLB, n=16; CHR-CBD, n=15; HC, n=19)

- A. Brain clusters showing linear relationship in encoding-related engagement, with activation being greatest (red/yellow) in the HC, lowest in the CHR-PLB and intermediate in the CHR-CBD. Clusters in blue/green display the opposite pattern of activation (CHR-PLB>CHR-CBD>HC).
- B. Brain clusters showing linear relationship in recall-related engagement, with activation being greatest (red/yellow) in the HC, lowest in the CHR-PLB and intermediate in the CHR-CBD. Clusters in blue/green display the opposite pattern of activation (CHR-PLB>CHR-CBD>HC).



## **eResults.**

### **Relationship between brain activation and symptoms:**

Post-hoc exploratory correlational analyses were carried out between psychopathology (as indexed by CAARMS positive and CAARMS negative subscales and STAI-S) and brain activation in CHR-PLB in the striatum, parahippocampal cortex and midbrain. Activation in the left caudate head during the encoding condition, which showed a linear relationship between the three groups of participants, with brain activation being greatest in the HC followed respectively by the CHR-CBD and CHR-PLB groups, was inversely correlated ( $r=-0.45$ ,  $p=0.039$ , 1-tailed) with CAARMS negative symptoms in CHR participants under the placebo condition (CHR-PLB). Activation in the midbrain, but not parahippocampal cortex during the recall condition, which showed a linear relationship between the three groups of participants, with brain activation being strongest in the HC followed respectively by the CHR-CBD and CHR-PLB groups, was inversely correlated ( $r=-0.40$ ,  $p=0.059$ , 1-tailed) with CAARMS positive symptoms and with STAI-S anxiety symptoms ( $r=-0.42$ ,  $p=0.053$ , 1-tailed) in the CHR-PLB participants.

**Adverse events:** No adverse or serious adverse events were observed in any of the CHR participants following single dose of study drug.

**eTable 1.** Task-related activation during the encoding condition relative to baseline in healthy controls (n = 19)

<b>Activation differences where Encoding &gt; Baseline</b>					
<b>Region</b>	<b>Coordinates of peak (TAL)</b>			<b>Cluster size</b>	<b>p value*</b>
	<b>X</b>	<b>Y</b>	<b>Z</b>		
Anterior cingulate	-14	41	-10	55	0.0081
Caudate body	21	-7	20	84	0.006
Precentral gyrus	-47	-11	30	71	0.006
Cuneus	0	-74	20	216	0.0013
<b>Activation differences where Encoding &lt; Baseline</b>					
Inferior temporal/ middle occipital gyrus	51	-56	-7	70	0.0084
Middle occipital gyrus	-36	-67	3	61	0.0088
Medial frontal gyrus	-4	55	7	55	0.0084
Inferior frontal gyrus	-58	18	-7	43	0.007
Middle frontal gyrus	36	37	10	248	0.001
Postcentral gyrus	54	-22	26	151	0.0014

TAL = Talairach coordinate system. \*Corrected for less than 1 false positive cluster.

**eTable 2.** Task-related activation during the recall condition relative to baseline in healthy controls (n = 19)

<b>Activation differences where Recall &gt; Baseline</b>					
<b>Region</b>	<b>Coordinates of peak (TAL)</b>			<b>Cluster size</b>	<b>p value*</b>
	<b>X</b>	<b>Y</b>	<b>Z</b>		
Parahippocampal gyrus	-18	-26	-13	103	0.0064
Transverse temporal gyrus	-47	-26	13	148	0.0046
<b>Activation differences where Recall &lt; Baseline</b>					
Middle occipital gyrus	-25	-85	-7	99	0.0086
Lingual gyrus	29	-70	-3	172	0.0049
Inferior frontal gyrus	47	14	23	140	0.0057

TAL = Talairach coordinate system. \*Corrected for less than 1 false positive cluster.

## **eDiscussion.**

Activation in CHR-PLB participants also differed from HC in other brain regions consistent with previous imaging studies comparing the two groups, though there were also areas where they differed from previous evidence (as reviewed here<sup>21-24</sup>).

Effect of a single dose of CBD on parahippocampal, midbrain and striatal activation is consistent with its potential role in amelioration of the neurophysiological abnormality that may underlie psychotic symptoms in CHR patients following longer-term treatment. In exploratory analyses, we observed an inverse relationship between the severity of positive psychotic and anxiety symptoms with activation in the midbrain and between the severity of negative symptoms with activation in the striatum in CHR-PLB participants. However, these relationships only showed trends towards statistical significance when examined at one-tailed significance threshold. Therefore, they should be interpreted with caution and are not discussed further.

## References.

1. Yung AR, Yuen HP, McGorry PD, et al. Mapping the onset of psychosis: the Comprehensive Assessment of At-Risk Mental States. *Aust N Z J Psychiatry*. 2005;39(11-12):964-971.
2. Spielberger CD. *Manual for the state/trait anxiety inventory (form Y) : (self evaluation questionnaire)*. Palo Alto: Consulting Psychologists Press; 1983.
3. Stafford MR, Jackson H, Mayo-Wilson E, Morrison AP, Kendall T. Early interventions to prevent psychosis: systematic review and meta-analysis. *BMJ*. 2013;346:f185.
4. Leucht S, Samara M, Heres S, Patel MX, Woods SW, Davis JM. Dose equivalents for second-generation antipsychotics: the minimum effective dose method. *Schizophr Bull*. 2014;40(2):314-326.
5. Leweke FM, Piomelli D, Pahlisch F, et al. Cannabidiol enhances anandamide signaling and alleviates psychotic symptoms of schizophrenia. *Transl Psychiatry*. 2012;2:e94.
6. Martin-Santos R, Crippa JA, Batalla A, et al. Acute effects of a single, oral dose of d9-tetrahydrocannabinol (THC) and cannabidiol (CBD) administration in healthy volunteers. *Curr Pharm Des*. 2012;18(32):4966-4979.
7. Bhattacharyya S, Fusar-Poli P, Borgwardt S, et al. Modulation of mediotemporal and ventrostriatal function in humans by Delta9-tetrahydrocannabinol: a neural basis for the effects of Cannabis sativa on learning and psychosis. *Arch Gen Psychiatry*. 2009;66(4):442-451.
8. Bhattacharyya S, Atakan Z, Martin-Santos R, et al. Preliminary report of biological basis of sensitivity to the effects of cannabis on psychosis: AKT1 and DAT1 genotype modulates the effects of delta-9-tetrahydrocannabinol on midbrain and striatal function. *Mol Psychiatry*. 2012;17(12):1152-1155.
9. Bhattacharyya S, Morrison PD, Fusar-Poli P, et al. Opposite effects of delta-9-tetrahydrocannabinol and cannabidiol on human brain function and psychopathology. *Neuropsychopharmacology*. 2010;35(3):764-774.
10. Coltheart M. The MRC Psycholinguistic Database. *Quarterly Journal of Experimental Psychology*. 1981;33A:497-505.
11. Kučera H, Francis WN. *Computational analysis of present-day American English*. Dartmouth Publishing Group; 1967.
12. Brammer MJ, Bullmore ET, Simmons A, et al. Generic brain activation mapping in functional magnetic resonance imaging: a nonparametric approach. *Magnetic resonance imaging*. 1997;15(7):763-770.
13. Thirion B, Pinel P, Meriaux S, Roche A, Dehaene S, Poline JB. Analysis of a large fMRI cohort: Statistical and methodological issues for group analyses. *NeuroImage*. 2007;35(1):105-120.
14. Hayasaka S, Nichols TE. Validating cluster size inference: random field and permutation methods. *NeuroImage*. 2003;20(4):2343-2356.
15. Bullmore ET, Brammer MJ, Rabe-Hesketh S, et al. Methods for diagnosis and treatment of stimulus-correlated motion in generic brain activation studies using fMRI. *Human brain mapping*. 1999;7(1):38-48.
16. Friman O, Borga M, Lundberg P, Knutsson H. Adaptive analysis of fMRI data. *NeuroImage*. 2003;19(3):837-845.



17. Bullmore E, Long C, Suckling J, et al. Colored noise and computational inference in neurophysiological (fMRI) time series analysis: resampling methods in time and wavelet domains. *Human brain mapping*. 2001;12(2):61-78.
18. Bullmore ET, Suckling J, Overmeyer S, Rabe-Hesketh S, Taylor E, Brammer MJ. Global, voxel, and cluster tests, by theory and permutation, for a difference between two groups of structural MR images of the brain. *IEEE transactions on medical imaging*. 1999;18(1):32-42.
19. Talairach J, Tournoux P. [*Co-planar Stereotaxic Atlas of the Human Brain*]. New York: Thieme Medical 1988.
20. Eklund A, Nichols TE, Knutsson H. Cluster failure: Why fMRI inferences for spatial extent have inflated false-positive rates. *Proc Natl Acad Sci U S A*. 2016;113(28):7900-7905.
21. Dutt A, Tseng HH, Fonville L, et al. Exploring neural dysfunction in 'clinical high risk' for psychosis: a quantitative review of fMRI studies. *J Psychiatr Res*. 2015;61:122-134.
22. Gifford G, Crossley N, Fusar-Poli P, et al. Using neuroimaging to help predict the onset of psychosis. *NeuroImage*. 2017;145(Pt B):209-217.
23. Hager BM, Keshavan MS. Neuroimaging Biomarkers for Psychosis. *Curr Behav Neurosci Rep*. 2015;2015:1-10.
24. Smieskova R, Fusar-Poli P, Allen P, et al. Neuroimaging predictors of transition to psychosis--a systematic review and meta-analysis. *Neurosci Biobehav Rev*. 2010;34(8):1207-1222.
25. Hawkins PCT, Wood TC, Vernon AC, et al. An investigation of regional cerebral blood flow and tissue structure changes after acute administration of antipsychotics in healthy male volunteers. *Human brain mapping*. 2018;39(1):319-331.
26. Lahti AC, Weiler MA, Medoff DR, Tamminga CA, Holcomb HH. Functional effects of single dose first- and second-generation antipsychotic administration in subjects with schizophrenia. *Psychiatry Res*. 2005;139(1):19-30.
27. McGuire P, Robson P, Cubala W, et al. Cannabidiol (CBD) as an adjunctive therapy in schizophrenia: a multicentre randomized controlled trial. *American Journal of Psychiatry*. 2017.
28. Simon AE, Cattapan-Ludewig K, Zmilacher S, et al. Cognitive functioning in the schizophrenia prodrome. *Schizophr Bull*. 2007;33(3):761-771.